Settlement due to Consolidation

H. Ohta
Research & Development Initiative, Chuo University, Tokyo, Japan
E-mail: ohta@tamacc.chuo-u.ac.jp

ABSTRACT: Settlement of the trial embankments placed on the campus of Asian Institute of Technology by (a) Akagi and (b) Ohta is discussed based on the performance of various settlement estimate techniques. Since these embankments were placed close to each other, mechanical parameters of the subsoil should be identical in both cases and therefore gives good chance to check the appropriateness and reliability of parameter estimation procedure. In addition to comparing the settlement estimate methods, proposed is a laboratory technique to estimate the in-situ effective stress state. This technique gives information on the change in effective stress state due to the progress of consolidation settlement.

Keywords: Consolidation, Settlement, Deformation, Soft clay.

1. INTRODUCTION

Passing away of the late Dr. Surachat Sambhandharaksa was the great loss to the community of geotechnical engineers not only in Thailand and Southeast Asia but also in the whole world. During the period of the author's stay in Rangsit in the early 80's working for Asian Institute of Technology, Dr. Surachat was always kind enough to take his valuable time for discussing with the author about various engineering problems mainly related to soft clays in Thailand. In this paper, the author introduces some of the geotechnical problems related to settlement due to consolidation that Dr. Surachat and the author seriously discussed in both the institute and the downtown.

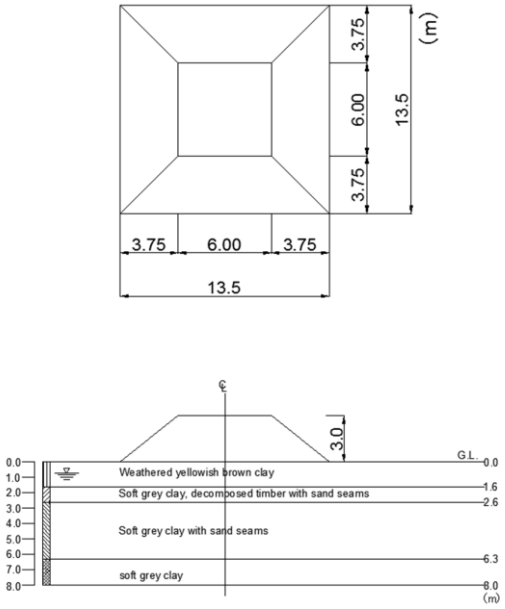

Figure 1 Akagi's trial embankment and subsoil profile

2. SETTLEMENT OF AKAGI'S TRIAL EMBANKMENT

2.1 General description

Two trial embankments were placed on the campus of AIT by Akagi (1981) during a period from 1979 to 1980. The embankments were square in their plan and constructed in two stages; first stage August-September 1979 (base width of 12 m, top width of 6 m, height of 2 m) and second stage January-February 1980 (base width of 13.5 m, top width of 6 m, height of 3 m) as shown in Figure 1. The average density of the fill body was 16.4 kN/m^3. General soil properties at the site are summarized in Figure 2.

The author has tried to analyse the settlement of one of these fills which was built on the natural ground having no artificial drainage facility such as sand drains. The settlement analyses were made using (1) Tezaghi's method usually employed in engineering practice. (2) Linearly elastic analysis, (3) Extended stress path method proposed by Poulos et al. (1976) based on the stress path method proposed by Lambe (1964), (4) Settlement prediction method proposed by Asaoka (1978), Asaoka and Matsuo (1979, 1980) based on the consolidation theory developed by Mikasa (1965) and (5) Soil/water coupled FE code DACSAR developed by Iizuka and Ohta (1982). These methods in predicting the consolidation settlement of the Akagi's embankment were compared to each other to see the difference between the methods.

The subsoil conditions, instrumentation for monitoring and performance of the embankments are fully described by Akagi (1981). The 1.5m thick surface crust of the ground is rich in fine cracks developed by the seasonal repetition of dry and wet processes. The surface crust consists of fill material placed on top of soft clay when AIT campus was built on the reclaimed land in the early 1970's. A soft layer of highly plastic clay lies at the depths between 2.5 and 8 m. A transient zone exists between the surface crust and the soft plastic clay. The seasonally fluctuating ground water table is at a depth of 0.45 m in the wet season and 2.3 m in the dry season. Fluctuation of the ground water table resulted in the over-consolidation ratio of 1.5~2.5 in the soft clay layer. The soft clay layer is underlain by yellowish stiff clay at about 8 m depth.

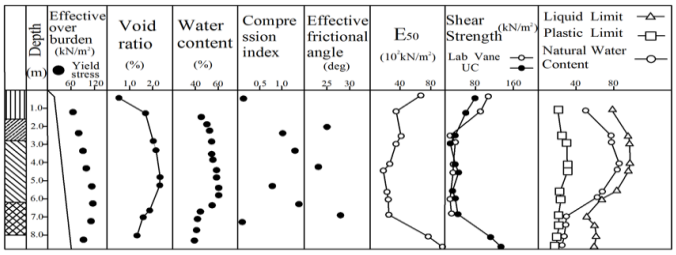

Figure 2 General soil properties at the site

2.2 Parameters used in the analyses

Table 1 lists the E_{50} obtained from unconfined compression tests on the 'undisturbed' samples of subsoil materials and Poisson's ratio. Deformability E_{50} of specimens at the stress level of half strength is expected to serve for Young's modulus. The Poisson's ratios are assumed as 1/3 instead of 1/2 that corresponds to undrained shear.

Table 1 Parameters used in linearly elastic analysis

Depth (m)	0.0－0.7	0.7－1.6	1.6－2.6	2.6－4.0	4.0－5.0	5.0－6.3	6.3－8.0
E_{50} (kN/m²)	6400	3600	3600	3600	2480	2480	2480
ν	1/3	1/3	1/3	1/3	1/3	1/3	1/3

The material parameters needed in the method proposed by Poulos et al. (1976) are obtained in the following procedure: (i) perform triaxial K_0-consolidation on the clay specimens sampled from mid-depth of clay layers applying the in-situ effective stress states estimated from the depth of underground water table, unit weight and K_0-value specified either experimentally or empirically, (ii) estimate the increments of the total stresses in the subsoil due to embankment loading by employing, for instance, the elasticity theory, (iii) apply the increment of total stress estimated in (ii) in addition to the in-situ effective stress state estimated in (i) under undrained conditions simulating the immediate deformation after embankment loading and obtain undrained deformability E_u, (iv) open the drainage cock allowing the consolidation to take place and obtain C_v and quasi-elastic parameters E' and ν', (v) continue to monitor the increasing deformation of the specimen after the consolidation process is practically completed to estimate the creep deformation and (vi) estimate the time-settlement curve based on the data obtained in the processes (i)-(v). The method of Poulos et al. needs complicated procedures of triaxial tests, but the logic is simple and easy to understand. Elastic parameters needed in the method of Poulos et al. obtained by a series of triaxial tests on clays under the Akagi's trial embankment are listed in Table 2 in which E_u is Young's modulus under undrained shear, E' and ν' are quasi-elastic parameters corresponding to Young's modulus and Poisson's ratio under fully drained shear (Molla, 1981).

Table 2 Parameters for Poulos et al. method

Depth (m)	0.0-1.50	1.50-3.75	3.75-5.75	5.75-8.00
Eu(kN/m²)	8040	3500	2910	3300
E'(kN/m²)	2520	970	897	772
ν'	0.42	0.34	0.28	0.28

Parameters needed in the observational method proposed by Asaoka (1978) are obtained from the settlement record monitored in some short period of about 10 days during embankment loading. Asaoka's method for the case of increasing load (Asaoka and Matsuo, 1980) is applied with some modification made by Galagoda (1981) in predicting time-settlement curve in the first stage of trial embankment (2 m high).

The parameters needed in the soil/water coupled FE code DACSAR are listed in Tables 3 and 4 in which soils A and B are assumed as elastic and C, D and E as elasto-plastic. Poisson's ratio for elasto-plastic materials is assumed as 1/3. The unit weight of compacted fill material is 16.4 kN/m^3. A constitutive model developed by Sekiguchi and Ohta (1977) is incorporated in the FE code DACSAR developed by Iizuka and Ohta (1982). DACSAR stands for "Deformation Analysis Considering Stress Anisotropy and Reorientation", but can also be read as "Dogs and Cats Search A Rat" implying that considerable efforts are needed in pursuing a relatively small gain. It should be noted that the permeability obtained from the laboratory (oedometer) tests are about 8 times smaller than the values which best fit with the time-settlement curve monitored in the field. This is a usual tendency most likely caused by the existence of thin sand seams in clay layers. In case of DACSAR analysis presented in this paper, the author used the input permeability 10 times larger than that obtained from the laboratory tests. By this the author intended to seek a round number to be multiplied to the lab permeability in our daily engineering practice.

Table 4 Parameters needed in DACSAR

	A	B	B	C	D	D	D	E
	1	2	3	4	5	6	7	8
Depth (m)	3.0～0.0	0.0～0.7	0.7～1.6	1.6～2.6	2.6～4.0	4.0～5.0	5.0～6.3	6.3～8.0
Lame λ	5.3×10^{-3}	5.3×10^{-3}	5.3×10^{-3}	—	—	—	—	—
Lame μ	2.6×10^{-3}	2.6×10^{-3}	2.6×10^{-3}	—	—	—	—	—
λ	—	—	—	0.35	0.52	0.43	0.39	0.30
μ	—	—	—	0.15	0.25	0.21	0.19	0.11
D	—	—	—	0.06	0.10	0.07	0.08	0.06
e_0	—	1.17	1.17	2.14	1.99	2.32	1.86	1.68
σ_{y0} (kN/m²)	—	—	—	74.7	77.5	91.8	106.5	91.0
σ_{yi} (kN/m²)	—	6.0	15.0	20.5	27.0	33.0	37.0	45.0
K_0	—	—	—	0.53	0.56	0.56	0.56	0.48
K_i	—	1.0	1.0	0.79	0.78	0.77	0.78	0.63
k (lab) (m/day)	1.0	1.4×10^{-4}	1.4×10^{-4}	3.9×10^{-4}	4.9×10^{-4}	4.9×10^{-4}	4.9×10^{-4}	1.1×10^{-4}
k(modified) (m/day)	1.0	1.4×10^{-4}	1.4×10^{-4}	3.9×10^{-3}	4.9×10^{-3}	4.9×10^{-3}	4.9×10^{-3}	1.1×10^{-3}

2.3 Comparison of analytical results with the field monitoring

Figure 3 demonstrates the performance of the analytical methods compared with the time-settlement curve monitored in the field. The Asaoka's method predicts the time-settlement curve almost identical with the monitored curve prior to the second stage of loading from the fill height of 2 m to 3 m, because the prediction is made based only on the observational information available from the settlement data in the first stage. Only a short period of observational time of about 10 days is found to be long enough to make highly reliable settlement prediction.

Table 3 Physical meaning of parameters needed in DACSAR

	Parameters	Main laboratory tests	Remarks
Material properties	λ compression index	Standard consolidation test, K_0 consolidation test	$\lambda=0.434C_c$
	κ swelling index	K_0 consolidation test	$\kappa=0.434C_s$
	D coefficient of dilatancy	Triaxial compression test	$M=\frac{\lambda-\kappa}{D(1+e_0)}$
Preconsol stress state	σ_{y0} preconsolidation pressure	Standard consolidation test, K_0 consolidation test	
	e_0 void ratio at preconsolidation	Standard consolidation test, K_0 consolidation test	
	K_0 coefficient of earth press, at rest	K_0 consolidation test	
Initial stress state	σ_{yi} effective overburden pressure	Unit weight test	$\sigma_{yi}=\gamma' z$, G.W.L
	K_i insitu coefficient of earth press, at rest	K_0 triaxial swelling test	
	k coefficient of permeability	Permeablity test, Standard consolidation test	$k=\gamma_w m_v C_v$

The Terzaghi's method and the Poulos et al. method based on the C_v obtained from the laboratory tests predict very slow progress of consolidation. However the Poulos et al. method using C_v which is 8 times larger than lab C_v produces very good results. It is expectable that the Terzaghi's method using the modified C_v will make very good prediction, too.

The DACSAR method produces the results in very good accordance with the monitored time-settlement curve when the permeability 10 times larger than laboratory permeability is used as the input parameter for the analysis.

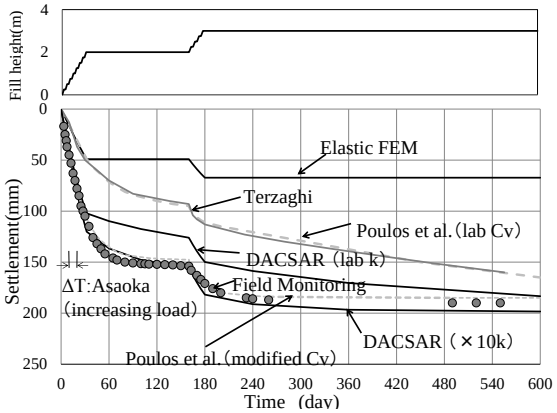

Figure 3 Performance of analytical methods

3. SETTLEMENT OF OHTA'S TRIAL EMBANKMENT

The author has placed a trial embankment on the campus of AIT during a period from October, 1980 to March, 1982 in vicinity of the Akagi's trial embankments. Figure 4 indicates the location of the embankment.

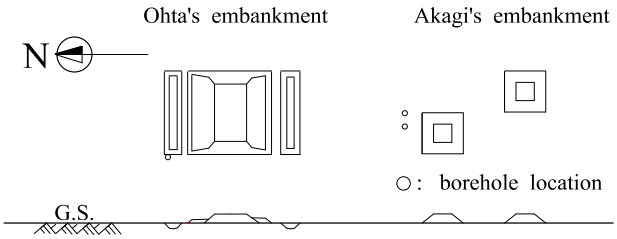

Figure 4 Location of the Akagi's and the Ohta's trial embankments

The construction work was performed as follows: (1) breakage of the tensile strength of the surface crust by digging 23 trenches (30 m long, 1.0 m wide and 1.5 m deep) at 4.0 m interval, (2) installation of monitoring instruments (14 deep settlement gauges and 14 open stand pipe piezometers being pushed into the soft clay layer from the bottom of the trenches and 3 dummy piezometers, 4 surface settlement plates and 17 ground surface stakes, 14 horizontal stakes and 4 bench marks), (3) construction of embankment (30 m long and 18m wide in base plane, 22 m long and 10.5 m wide in top plane and 2.8 m high with a slope of 3:4) started on 18th March and finished on 22nd March, 1981 (18th: 0~0.5 m, 19th: 0.5~1.0 m, 20th: 1.0~2.0 m, 21st: 2.0~2.4 m and 22nd: 2.4~2.8 m, average unit weight of compacted fill : 13.8 kN/m^3), (4) excavation near the toes of the embankment allowing further lateral movement of the soft foundation (trenches of 6 m x 30 m on the top plane and 2 m x 30 m on the bottom plane, 1.9 m deep) together with additional loading by placing the excavated soil alongside the slopes of the existing embankment to form berms on both sides of the embankment. (Excavation works started on 23rd November (as Day 251) and completed on 24th November, 1981 on the northern side of the fill and started on 23rd December, 1981 and completed on 24th December, 1981 on the southern side of the fill.)

The author called the steps (1) through (3) as the Phase I and the step (4) as the Phase II. Figure 5 (a) - (h) show the construction works going on with the activities performed by then students. Figure 6 shows the cross section of the fill during Phase I and II.

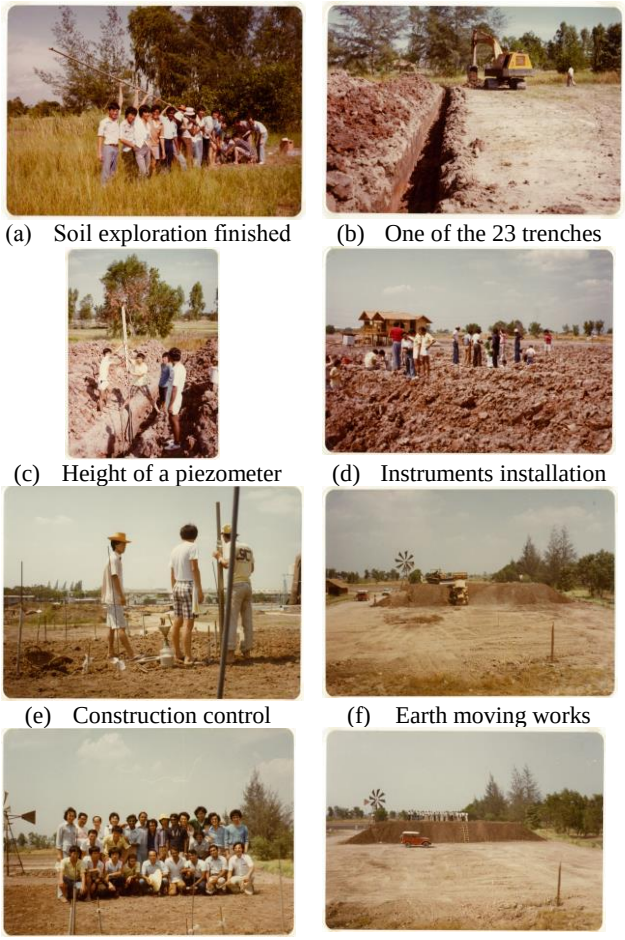

(a) Soil exploration finished (b) One of the 23 trenches

(c) Height of a piezometer (d) Instruments installation

(e) Construction control (f) Earth moving works

(g) Students involved (h) Embankment completed

Figure 5 Construction works of the Phase I

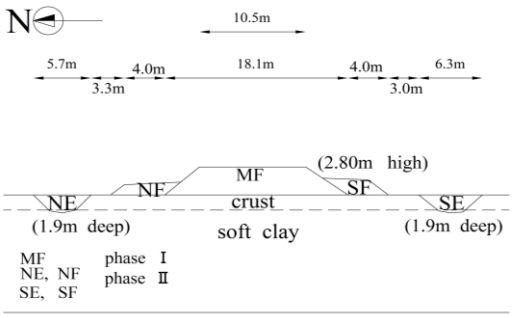

Figure 6 Cross section of Ohta's embankment and excavation

Ideally, the excavation work should be carried out by removing a thin layer of soil one after another until reaching a depth of 1.9 m so that the stress changes approximate the plane strain condition. However, actually, this was not convenient from the construction point of view. Thus, piece-wise excavation from the west to the east was performed. The unfavourable movement, that is the gradual progress of deformation of the embankment from one side to the other, was to be neglected in the analysis. In the same way the excavation in south side began on 23rd December (as Day 283) and completed on 24th December, 1981. The excavated soil was put to form a rhombic fill alongside the trial embankment forming a kind of berms on both sides (Figure 7). Details of instrumentation prior to the construction of embankment are described by Ho (1982) and Ohta and Ho (1982).

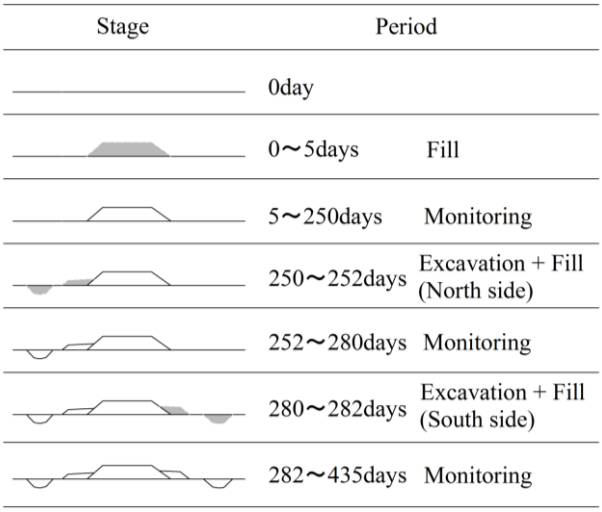

Figure 7 Construction sequence in Phase I - II

The project further went on to the Phase III during a period from 31st May to 25th June, 1982 to increase the height of the fill additionally 1.0 m aiming at bringing the embankment into a state of further instability and planned to cause failure in Phase IV. But those stages will not be described in this paper because it becomes too lengthy.

Since no effort had gone into analysing the performance of the Ohta's embankment using the DACSAR code, the author started analysing it in preparing this paper by employing the DACSAR code developed by Iizuka and Ohta (1987). The parameters used in the analysis are identical with those listed in Table 4.

Figures 8 and 9 indicate the location of the settlement gauze SSG12 and its settlement records compared with the DACSAR analyses using (i) the permeability coefficient k obtained from the oedometer tests in the laboratory and (ii) the one 10 times larger than the lab k for the soft clay layer. Figure 10 shows the change in settlement profile with the elapsed time.

The analytical settlement curves shown in Figure 9 do not fit very well with the settlement records monitored in the field at a point of the settlement gauze SSG12. The cross sectional profiles of monitored settlement shown in Figure 10 are not in very good agreement with the analytical profiles, too. This is in contrast to the very good agreement shown in Figure 3 which was made using exactly identical set of input parameters indicating the need of further investigation of parameter specification procedures. As is implied in Figures 3 and 9, the apparent rate of consolidation settlement is largely governed by the overall permeability of soft clays.

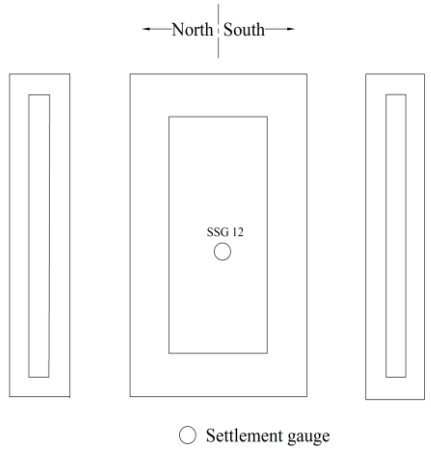

Figure 8 Location of the settlement gauze SSG12

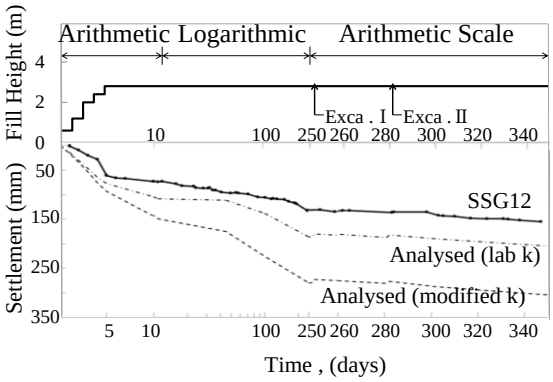

Figure 9 Settlement records at SSG12 compared with the settlement computed by using DACSAR

It is well known that the permeability of a clay layer is several times different for the water flows in vertical and horizontal directions. It is also well known that the permeability of a clay layer largely depends, by a logarithmic scale, on the effective stress state. It is widely recognised that the existence of sand seams and sand lens in a clay layer can potentially influence on the permeability usually estimated by carrying out oedometer tests on clay specimens trimmed intentionally avoiding the sand particles in clusters in the clay being trimmed. We all know that many factors influence on the estimate of permeability of clays and yet we do not fully know how we can reliably estimate the permeability.

The author had many occasions of seriously discussing about those issues with Dr. Surachat. They enjoyed the discussion but did not find any drastic solutions.

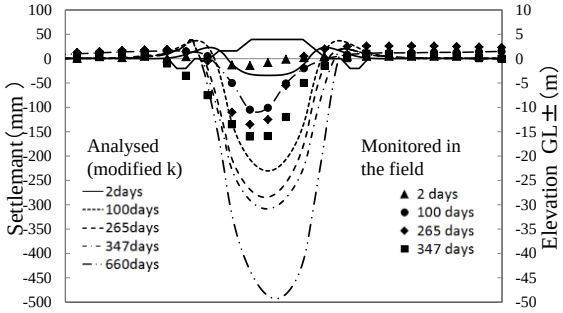

Figure 10 Settlement profile changing with elapsed time

4. ESTIMATE OF IN-SITU EFFECTIVE STRESS STATE

4.1 Negative pore pressure in "undisturbed" clay samples

Usual process of taking so-called "undisturbed" samples from soft clay layers using thin-walled tubes is actually more complicated than that shown in Figure 11 in which the simplified concept of sampling process starts from stage A where a clay element sits deep under the ground and moves to the following stages: B sampling by taking the clay element into a sampler, C extrusion of the clay from the sampler, D trimming the specimen and E testing.

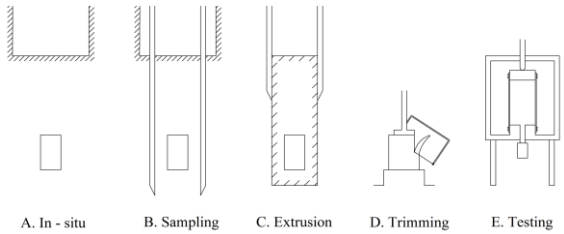

Figure 11 Simplified process of sampling "undisturbed" clay

"Undisturbed" samples before being taken from the bottoms of bore-holes still remain in the effective stress state as they were before boring operations start (stage A in Figure 11). The in-situ effective stress state of the "undisturbed" sample at stage A is typically represented by point A_e in Figure 12 in case of normally consolidated clays for which the value of the coefficient of earth pressure at rest Ko (=effective horizontal stress / effective vertical stress) is in a range of 0.4~0.7. Since the total stress state is obtained by adding in-situ (usually hydrostatic) pore water pressure to both of the effective vertical and horizontal stresses, the in-situ total stress state at stage A is represented by point A_t in Figure 12. At stage B in Figure 11, the "undisturbed" sample is taken into the sampler, separated from the clay deposit immediately beneath it by application of suction force and lifted up to the ground surface. During these processes of handling the "undisturbed" sample, both the effective and total stress states (B_e and B_t in Figure 12) are ideally supposed to stay at the in-situ stress states and remain unchanged with the help of wall-cohesion. This "ideal" assumption of no stress change during the sampling process (stage B) may not be close to what really happens to the "undisturbed" sample at stage B but we have no reliable means of estimating the actually induced stress change.

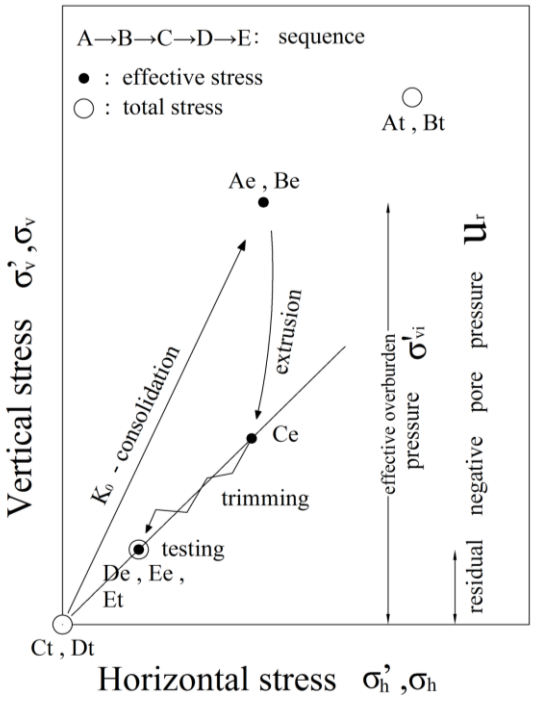

Figure 12 Stress change experienced during stages A~E by a "undisturbed" sample of normally consolidated clay

The "undisturbed" sample lifted up to the ground surface is carried to the laboratory and extruded from the sampling tube (stage C in Figure 11) being exposed to the atmospheric pressure under which both the vertical and horizontal total stresses are zero (point C_t in Figure 12). The change in the total stress state from the in-situ anisotropic Ko state to the isotropic state in the laboratory forces the "undisturbed" sample into undergoing undrained extension whose effective stress path is indicated by a curved arrow starting from point B_e and ending at point C_e in Figure 12. Undrained extension of the "undisturbed" sample during the process of extrusion induces negative pore pressure by amount of difference of ordinates (and/or abscissas) of point C_e and point C_t. The sample then undergoes the trimming process (stage D in Figure 11) during which total stress of the sample stays at point D_t in Figure 12 while effective stress moves from C_e to D_e due to the disturbance caused by cutting and trimming operations. The axial strain needed in bringing undisturbed clay samples to the failure state is generally of the order of a few percent. And it is likely to happen during poorly performed trimming process that we force our clay samples to deform to a degree comparable to this failure level and produce pore pressure as much as shown by the difference of ordinates (and/or abscissas) between points C_e and D_e. During the trimming process, total stress state of the sample remains unchanged and stays at point D_t as shown in Figure 12. Thus the trimming process decreases the negative pore pressure in the "undisturbed" sample to a level that we call the residual negative pore pressure u_r.

At stage E in Figure 11, the sample is ready to undergo, for instance, triaxial or oedometer tests under the effective initial stress state represented by E_e in Figure 12. In the figure, the total stress point of the sample prior to testing is shown as E_t as a typical case of triaxial consolidated-undrained test. It inevitably takes place that some amount of air gets into the sample and also remains to exist in the gap between the sample and the rubber membrane during the process of trimming and preparation for testing (stages D and E in Figure 11) making the pore pressure measurement less accurate.

Figure 13 shows the process of stress changes experienced by a lightly over-consolidated clay sample in the similar fashion shown in Figure 12. The in-situ effective stress state represented by A_e and B_e in Figure 13 is somewhat different from those in Figure 12 due to the overconsolidation. In case of O. C. clays, the elastic response during extrusion (undrained extension) process plays an important role in sharp contrast to the case of N. C. clays resulting in relatively higher ratio of u_r / σ_{vi}' .

Figures 12 and 13 are schematically produced based on the ideas fully described by Skempton and Sowa (1963), Ladd and Lambe (1964) and Noorany and Seed (1965).

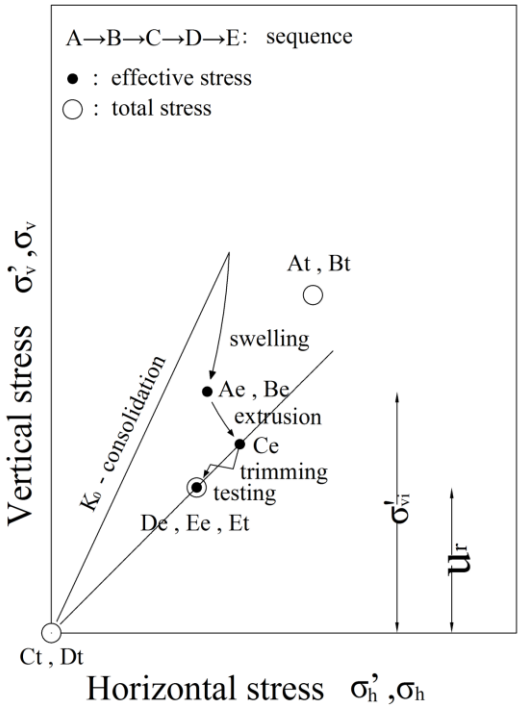

Figure 13 Stress change experienced during stages A~E by a "undisturbed" sample of lightly overconsolidated clay

4.2 Measurement of residual negative pore pressure

As demonstrated in Figures 12 and 13, the total and effective stress states in a specimen of "undisturbed" clay placed on the pedestal in a triaxial chamber are represented by D_t and D_e. Magnitude of residual negative pore pressure u_r being kept in the specimen at this stage is given by amount of difference of ordinates (and/or abscissas) of point D_e and D_t when the cell pressure is zero. If the cell pressure starts gradually increasing under undrained conditions, the "ideal" pore pressure response monitored by using an ideally accurate transducer (which can accurately measure pore pressure both in positive and in negative values even when we have air bubbles in and around the specimen) should be as indicated by open circles ○ in Figure 14. The open circle ○ located just on the axis of ordinates indicates the absolute value of the residual negative pore pressure existing in the specimen at the stage of starting triaxial testing.

If a sort of "perfect" transducer (which can accurately measure only when pore pressure is positive under conditions of air bubble existence) instead of an above mentioned "ideal" transducer is used, monitored pore pressure response should be the data represented by solid circles ● in Figure 14. The solid circle ● moves upward along the axis of ordinates while the negative pore pressure still remains as negative at the early stage of application of gradually increasing cell pressure and suddenly starts moving toward the right upward direction following the open circles ○ making a sharp kink of the path at the point where the applied cell pressure reaches as high as the absolute value of the residual negative pore pressure that existed in the specimen at the starting stage of triaxial testing. It is thus possible to measure negative pore pressure in the specimen by using either "ideal" or "perfect" pressure transducers.

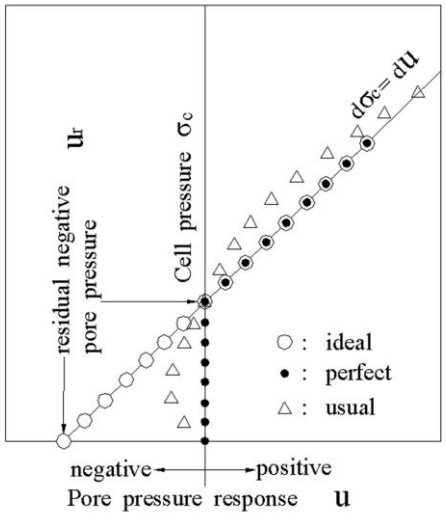

Figure 14 Pore pressure response to the gradual increase of cell pressure

However, unfortunately no "ideal" or "perfect" transducers are available as a matter of fact. We have no choice other than using "usual" transducer which is not able to measure negative pore pressure and is strongly time dependent in responding to changing pore pressure especially when air bubbles exist in the measuring system. The pore pressure response monitored by using "usual" transducer looks most likely as shown in Figure 14 by open triangles △. The open triangle △ moves from the lower centre of Figure 14 toward left upward direction in the early stage of the increase of the cell pressure indicating the real pore pressure must be somewhat higher (to further negative direction) than the open triangles △. Then the monitored pore pressure starts increasing with further increase in the cell pressure and move toward right upward as shown in Figure 14. It should be noted that thus measured values of pore pressure represented by open triangles △ are smaller in their absolute values than the pore pressure actually existing in the specimen (represented by open circles ○ in Figure 14) no matter whether the pore pressure is positive or negative. Even in case that usual transducers are employed, theoretically it is possible to find out the absolute value of the residual negative pore pressure as the value of cell pressure at the stage when the measured value of pore pressure becomes again as zero. However this is not practically reliable and is not used in this paper.

Figure 15 shows the experimental technique how to find out the residual negative pore pressure remaining in the specimen of "undisturbed" sample placed on the pedestal of a triaxial chamber. It should be noted that the pressure transducer employed in this experiment is of just a usual type, neither "ideal" nor "perfect" transducers. The transducer cannot measure the negative pore water pressure accurately and has strong time dependency in responding to the changing pore pressure mainly caused by the creep behaviour of clays in addition to the effect of existence of air bubbles in the measuring system.

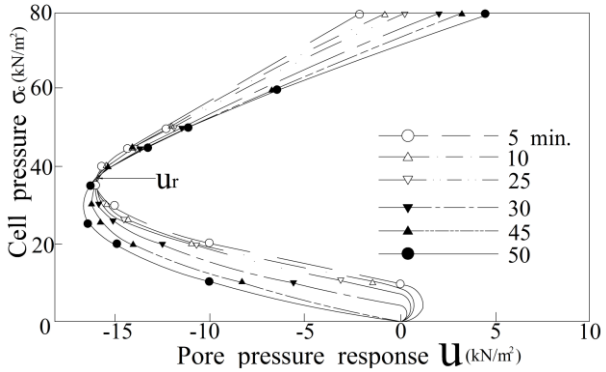

Figure 15 Negative pore pressure measurement using a newly developed experimental technique

In applying this method, the specimen covered by a thin rubber membrane is placed on the pedestal of a triaxial chamber with the drainage line being closed. The all-round cell pressure is applied stepwise with a certain time interval. During this time interval, the pore pressure response measured by the pressure transducer changes with time. In the case shown in Figure 15, the first step of applied cell pressure (10 kN/m^2) is maintained for 50 minutes. The pore pressure measured by the transducer is about zero at the elapsed time of 5 minutes. It decreases with the elapsed time of 10, 25, 30, 45 minutes and reaches about -10 kN/m^2 at the elapsed time of 50 minutes. As mentioned above, this is the effect of time lag in measuring the pore pressure, arising partly from the existence of air bubbles in the measuring line and partly from the viscous nature of clays.

The pore pressure measured by the transducer tends to decrease while the cell pressure is in some lower levels. When the cell pressure exceeds a certain level, the pore pressure response turns to increase with time. In the case shown in Figure 15, the cell pressure at the turning point is read as about 35 kN/m^2. The absolute value of pore pressure measured by the transducer must be doubtful, since the usual type of transducer is not reliable in measuring the negative pore pressure. The absolute value of the residual negative pore pressure (and therefore the residual effective stress remaining in the specimen immediately before testing) specified by employing the present technique is identical with the cell pressure at the turning point of pore pressure response from decreasing to increasing tendency. In the case shown in Figure 15, it is about 35 kN/m^2 indicating that the residual effective stress remaining in the specimen immediately before testing was about 35 kN/m^2.

The response of pore pressure transducers tends to move with elapsed time toward the value of pore pressure actually existing in the specimen. The principle of the present technique is that the pore pressure measured by the transducer should not change its value with time when the applied cell pressure happens to be identical with the residual effective stress in the specimen resulting in the zero pore pressure. The method essentially relies on the time lag characteristics of usual transducers. In the case shown in Figure 15, the time interval of stepwise increase of the cell pressure is 50 minutes. After making some trials, it was found that stepwise rise of the cell pressure at the time of 1, 2, 4, 8 and 15 minutes is long enough to specify the cell pressure with no change of transducer response. The time interval for this shortened version of testing is 1, 2, 4 and 7 minutes at each step. This shorten version of testing needs about 2 hours (=15minutes x 8 levels of applied cell pressure). Details of experimental procedure are fully described by Empig (1981).

4.3 Case records of measuring residual negative pore pressure in "undisturbed" clay samples taken from 3 sites

Figure 16 shows the residual effective stresses remaining in "undisturbed" samples taken from a lightly overconsolidated clay deposit. The residual effective stress is identical in its absolute value with residual negative pore pressure which is experimentally specified by means of technique introduced in the previous section. Since the overconsolidation ratio is in a range of 1~1.2 for the clay shallower than 30 m, "undisturbed" samples taken from this site are supposed to have experienced the process described in Figure 12. As seen in Figure 16, the residual effective stresses are about 20% of the effective overburden pressure at the site. This seems to be in reasonable accordance with the expectation based on Figure 12.

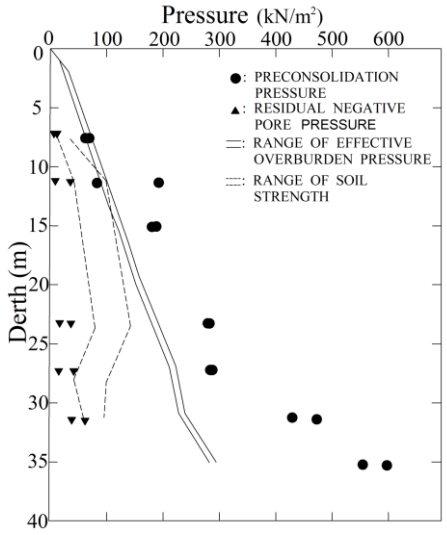

Figure 16 Residual effective stresses in "undisturbed" clay samples taken from a lightly overconsolidated clay deposit

Figure 17 shows another record of residual effective stresses remaining in "undisturbed" samples taken from the site in AIT. "Undisturbed" samples were taken from two boreholes; one bored at the centre of the Akagi's embankment shown in Figure 1 and the other at the location somewhat remote from the Akagi's embankment but not too far from it. The author expected to find some clear evidence of the consolidation due to the weight of the embankment, since the consolidation has already been at the final stage when the author made those two boreholes.

As seen in Figure 2, the overconsolidation ratio of the clay is around 2 implying the stress history followed by the clay outside the area loaded by the embankment is similar to the one shown in Figure 13.

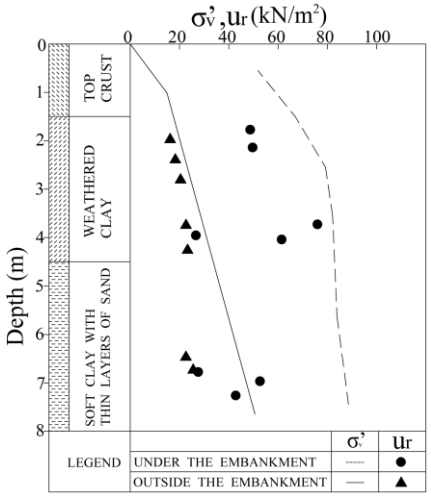

Figure 17 Residual effective stresses of clays under and around the Akagi's embankment

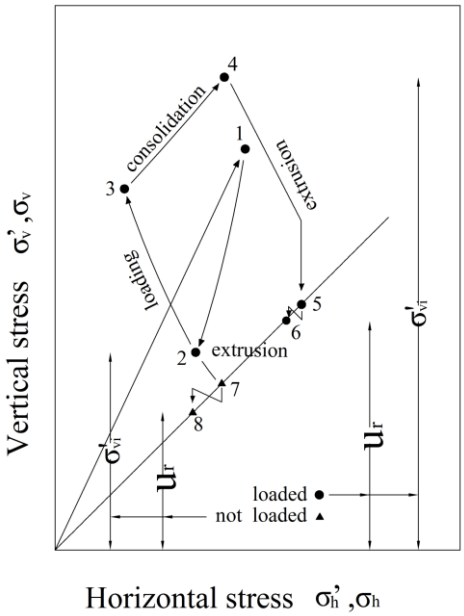

Figure 18 Stress change experienced by "undisturbed" clays loaded and not loaded by the Akagi's embankment

The stress history probably experienced by the clay under the embankment is schematically shown in Figure 18 where the original effective stress state of the overconsolidated clay (point 2 in Figure 18) moves to point 3 due to the immediate loading by the embankment followed by the increase in the effective stress due to consolidation (point 4). The clay was taken from the site and extruded from the sampling tube resulting in the effective stress state represented by point 5. The sample was trimmed and reached the state of point 6. The ordinates of point 4 and point 6 are the estimated in-situ effective overburden pressure and the residual negative pore pressure (and therefore residual effective stress) respectively. For the clay taken from outside of the loaded area, the original effective stress state (point 2) moves to point 7 and eventually to point 8. From the relative location of these effective stress points, the author expected to have the residual effective stresses in the "undisturbed" samples much higher than those shown in Figure 16. The data points plotted in Figure 17 are generally in good accordance with the expectation except a few data points of the clay at a depth around 7 m where we had thin layers of sand.

Two sets of data point plotted in Figure 17 clearly indicate that the measurement of the residual negative pore pressure (and therefore residual effective stress) can present undeniably obvious evidence of the occurrence of consolidation in clay layers. Dr. Surachat joined the author in supervising a postgraduate student on the subject of residual negative pore pressure introduced in this section. They had a lot of discussion making themselves confident that the method produces reasonable results. It still remains in the author's mind as nice memory with Dr. Surachat.

Figure 19 shows the residual effective stress in "undisturbed" samples taken from two boreholes; one drilled at the centre of the basement of a high-rise building under construction and other outside the building area at a distance of about 100 m from the building. The building was at a final stage of construction and the weight of the heavy building was already transmitted to a firm layer of fine sand on which the foundation of the building rested as shown schematically in Figure 19. The purpose of sampling was to find out the reason of the unexpected settlement of the building. The author has drilled above mentioned two boreholes by himself and carefully took "undisturbed" samples.

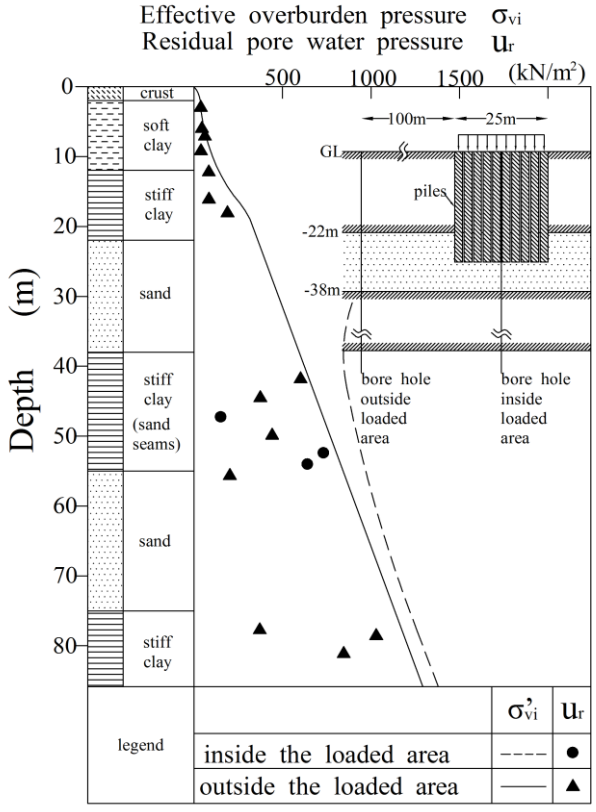

Figure 19 Residual effective stresses remaining in "undisturbed" samples taken from two areas loaded and not loaded by the heavy high-rise building

The heavy weight of the building increases the effective vertical stress in the stiff clay layer (at depth of 38 m ~ 54 m) immediately beneath the sand layer (at depth of 22 m ~ 38 m) as much as shown by a dotted curve in Figure 19 if the excess pore pressure induced by the building load is completely dissipated. Since the stiff clay layer is supposed to be lightly overconsolidated, there are two possible stress changes experienced by the "undisturbed" samples taken from beneath the building such as shown in Figure 20.

In case that the excess pore pressure possibly induced by the building load does not have enough time to dissipated or in case that the stiff clay layer does not receive any appreciable stress increase due to the building load, initial effective stress state (point 1) moves to point 6 either by passing through point 2 (i.e. no time for the excess pore pressure to dissipate) or directly from point 1 to point 6 (i.e. no appreciable load increase). In these cases, the measured residual pore pressure should be much smaller than the initial effective overburden pressure (i.e. small value of ratio of u_r/σ_{vi}') as demonstrated in Figure 20 as the case of "short term".

On the other hand, in case that the excess pore pressure due to building load is completely dissipated, point 1 moves to point 2 and then moves to point 3 with the progress of consolidation and eventually reaches point 5 resulting in the ratio of u_r/σ_{vi}' which is higher than the other cases as indicated by "long term" in Figure 20. Measured values of residual negative pore pressure in the stiff clay layer immediately beneath the sand layer plotted in Figure 19 are not too low compared with the effective overburden pressure implying in a vague way that the clay layer is already consolidated by the building load.

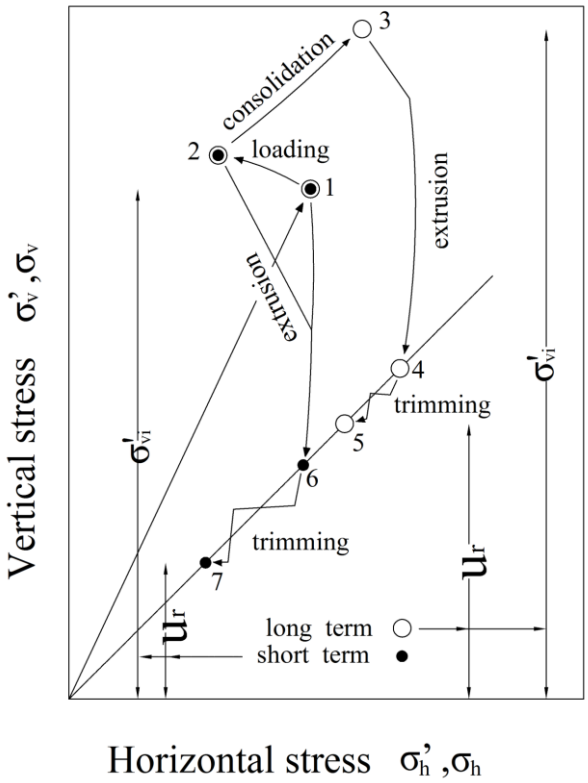

Figure 20 Two possible effective stress changes experienced by "undisturbed" samples under the building

The author had a lot of discussion with Dr. Surachat about the possible interpretation of the data points plotted in Figure 19. After discussing a lot, the author eventually had a thought to compare the water content of the clays taken from inside and outside of the building. It was striking to the author to find out a simple fact that the water contents of the clay samples at depth 38 m ~ 54 m inside the building were a few percent, if the author remembers correctly, lower than those of outside area. Integration of thus found difference of the water content throughout the layer happened to be equivalent to the amount of settlement of the building. It is a pity that those raw data are missing and the author cannot find them after spending about 35 years. It was disappointing to the author to find out that such a simple method of comparing the water content was much more reliable and explanatory than the measurement of residual negative pressure to which the author and Dr. Surachat paid much effort and time.

5. PARAMETER DETERMINATION PROCESDURES

In his trials of solving geotechnical problems in Thailand, Dr. Surachat tried to understand what was/is or will be going on at the sites based on the latest knowledge of geotechnical engineering such as anisotropic strength of natural clays under undrained shear. However the design techniques widely accepted in the engineering practice were of traditional methods in which the new knowledge such as strength anisotropy etc. is not taken into account. How to fill the gap between the new geotechnical findings and the traditional way of understanding was often discussed by Dr. Surachat and the author. In this section the author introduces some of the test results which imply that we still need more investigations to improve our current procedures to determine the soil parameters closely related to the estimate of settlement and deformation of the ground.

Figure 21 shows an interesting example of the preconsolidation pressures estimated by various reporters. The author's oedometer test results (Ohta and Ho, 1982) in agreement with Rahman's findings (1980) indicate that the preconsolidation pressures are small in the shallow area down to a depth of 3.5 m with increasing tendency with depth. However, down to a depth of 3.5 m, the preconsolidation pressures reported by the previous investigators (Kanjanophas (1969), Kangsasitiam (1970), Kim (1970), Kang (1970), Pham (1972), Prapaitrakul (1975), Taesiri (1976) and Dumn Muh (1977)) indicate a contrary tendency. This implies that the apparent preconsolidation pressure has decreased in the top layer of the clay sometime during a period between 1970-1980. There is no reasonable explanation for this change to the author's best knowledge.

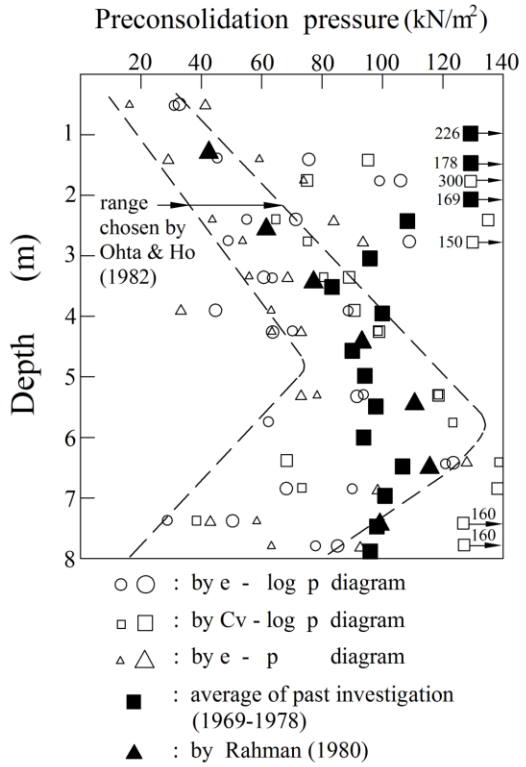

Figure 21 Preconsolidation pressure estimated by
(i) two series of oedometer tests by Ohta and Ho (1982) (open circles, squares and triangles) ,
(ii) average of past investigations performed at AIT (solid squares) by Kanjanophas (1969), Kangsasitiam (1970), Kim (1970), Kang (1970), Pham (1972), Prapaitrakul (1975), Taesiri (1976) and Dumn Muh (1977)
(iii) Rahman (1980) (solid triangles)

There are three different ways of specifying the preconsolidation pressure based on the oedometer tests plotted on: (i) e-log p diagram, (ii) C_v-log p diagram and (iii) e-p diagram. The preconsolidation pressure is defined as the point of sharp kink in those diagrams. The origin of the idea is common in these three different ways that is the sharp change in compressibility with the increase in consolidation pressure. When the applied pressure exceeds the preconsolidation pressure, e and C_v changes drastically. We should expect the same value of preconsolidation pressure obtained from these three ways because all of them are based on the change in the compressibility of the clay. However, as seen in Figure 21, there exists considerable difference of the preconsolidation pressure estimated by these three different ways.

Ohta and Ho (1982) have chosen a band as the possible range of preconsolidation pressure as indicated by dotted curves in Figure 21. As well understood by all of geotechnical engineers, the value of preconsolidation pressure is largely influential in estimating the consolidation settlement. And yet there is no clear criterion of choosing a representative value from the area specified by the band. This means that we can choose a representative value of the preconsolidation pressure with some considerable arbitrariness in such a way that the computed settlement fits well with the observed one in case that the observation is made prior to the computation.

Table 4 shows 9 undisturbed samples subjected to consolidated-undrained triaxial testing. Newly developed triaxial testing apparatus is used in a series of testing as introduced by Nakayama et al. (2013), Takeyama et al. (2014) and Kobayashi et al. (2014) to see the effect of strain rate on the effective stress paths and stress-strain relationships.

Table 4 Undisturbed clay samples subjected to consolidated undrained triaxial testing

No.	Site	Depth (m)	Axial strain rate %/min	Natural water content w (%)	Plasticity index I_p	Clay fraction under 2μm (%)
①	Saitama	GL -11.50 ~ -	0.05	33.9	16.5	8
②	Urayasu	GL -29.00 ~ -	0.05	66.3	54.4	36
③	Urayasu	GL -22.00 ~ -	0.05	58.4	54.8	32
④	Saitama	GL -11.50 ~ -	0.005	41.0	27.0	8
⑤	Urayasu	GL -29.00 ~ -	0.005	27.5	11.6	10
⑥	Urayasu	GL -22.00 ~ -	0.005	66.8	61.2	37
⑦	Hiroshima	GL -21.50 ~ -	0.05	82.0	85.7	70
⑧	Hiroshima	GL -21.50 ~ -	0.005	81.7	82.2	69
⑨	Saitama	GL -29.00 ~ -	0.005	114.2	53.1	54

Figure 22 demonstrates the effect of the shearing rate on the effective stress paths and the stress-strain relations of clays subjected to the consolidated-undrained compression tests. Appreciable influence of the strain rate is seen on the deformability of clays. The loading period at the sites caused by construction activities is usually of the order of several months or more and the strain rate that clays experience at the sites is much slower than 0.05~0.005%/min. This implies that the material parameters estimated based on the standard triaxial undrained shear need some correction of shearing rate.

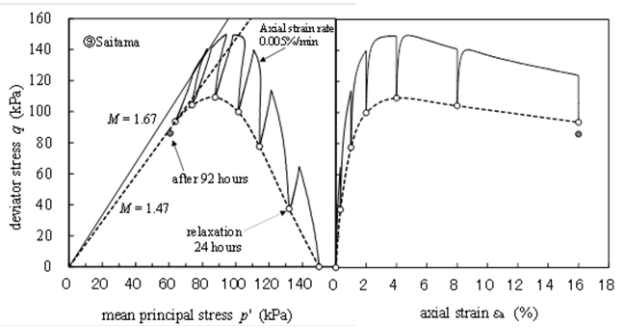

Figure 22 Consolidated undrained tests on undisturbed clay samples (No. 1 through No. 8 in Table 4) sheared under standard and slow rate of shearing

Figure 23 shows the results of consolidated-undrained test with stepwise relaxation in which the increase in axial strain stops for 24 hours keeping the axial strain unchanged. The strain rate during loading is 0.005%/min. This means that the obtained stress path and stress-strain relation after stress relaxation (shown by dotted curves in Figure 23) correspond to very slow loading rate that the clay may experience at the site of construction works. Apparently the rigidity of the clay sheared with the strain rate of 0.005%/min is much higher (i.e. stiffer) than the rigidity observed after stress relaxation.

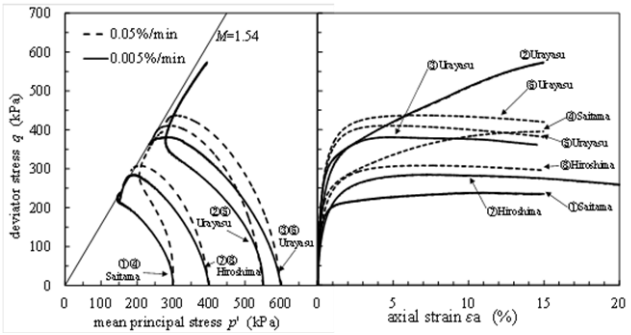

Figure 23 Consolidated undrained test with stepwise stress relaxation on clay (No. 9 in Table 4)

The tests results shown in Figures 22 and 23 imply that the stress-strain characteristics of undisturbed clay samples are largely influenced by the strain rate of testing which is usually much faster in the laboratory than the strain rate experienced by the clay loaded due to the construction activities at the site. From this point of view, triaxial tests in the laboratory should be performed with the strain rate much slower than 0.05%/min which is the standard strain rate adopted in the Japanese engineering practice. However, on the contrary, it is also needed to carry out triaxial tests within a certain time period from the economical viewpoint. To resolve this apparent contradiction, we need further investigation on, for instance, the correction factors.

6. CONCLUDING REMARKS

During the whole period of his service to Asian Institute of Technology, the author had very nice time with Dr. Surachat and enjoyed trying to produce something new related to consolidation settlement together with him. Conclusions drawn from those trials introduced in this paper are as follows.

Employment of the finite element method using a linearly elastic stress-strain relation in terms of total stress in estimating the consolidation settlement needs careful attention in specifying the elastic parameters of the subsoils. The usage of E_{50} as the substitute of the Young's modulus did not work well as shown in Figure 3.

The Terzaghi's method, the Extended Stress Path Method proposed by Poulos, Ambrosis and Davis (1976) and the soil/water coupled FEM code DACSAR developed by Iizuka and Ohta (1982, 1987) work well for the case of the Akagi's embankment under conditions that proper method of estimating the C_v or k representing the overall permeability of the subsoils is known based on the past experience at the site. However DACSAR produced the estimate of the consolidation settlement of the Ohta's embankment not as good as for the Akagi's embankment even though the material parameters used in the computation of both cases are identical.

The observational method proposed by Asaoka (1978), Asaoka and Matsuo (1979, 1980) works very well even in the case that the period of observation is very short.

A new experimental technique of measuring the residual negative pore pressure remaining in "undisturbed" clay samples is proposed by the author in this paper. Since the effective stress state is estimated based on the measured residual negative pore pressure under conditions of the atmospheric zero total stress, the in-situ effective stress state can be vaguely known giving the idea, at least theoretically, of the degree of consolidation which is going on at the site. Performance of this technique applied to 3 sites implies that it works reasonably well. However it was finally found that the measurement of the water contents of "undisturbed" samples is much more reliable and explanatory than the complicated measurement of the residual negative pore pressure remaining in the "undisturbed" samples.

In order to achieve more reliable estimate of the settlement and deformation of the ground loaded by external agencies, further investigation on the parameter determination procedures is needed.

7. ACKNOWLEDGEMENTS

The author wishes to express his profound gratitude to then students of AIT Mr. Md. Koramat Ali Molla, Mr. H. M. M. B. Galagoda, Mr. Vicente E. Empig, Mr. Rhee Yong-Heun, Mr. Samuel Handali, Mr. Tsai Chow-Yuan, Mr. Chartri Asavaratanaporn, Dr. Wanchai Teparaksa and the late Dr. Ho Yu-Chen for their cooperation in carrying the research projects introduced in this paper. They were outstandingly excellent students comfortable to work with. Also special thanks are extended to the author's former colleagues at AIT, Prof. A. S. Balasubramaniam, Prof. Yudhbir, Prof. Prinya Nutalaya, Dr. R. Peter Brenner, the late Dr. Andrea Tomiolo, Dr. Jerasak Premchit, Dr. Friedrich Prinzl and Prof. Worsak Kanok-Nukulchai.

The author would like to acknowledge the support and encouragement given to him by Dr. Suched Likitlersuang, Editor-in-Chief of Special Issue *Advances in geotechnical Engineering for Infrastructure Developments in Thailand.* Figures and tables in this paper were reproduced with the help of Dr. Yukio Arai and Mr. Kazuki Ogawa, Asano Taiseikiso Engineering Co. Ltd. Their support is deeply appreciated. This work was partly supported by JSPS Grant-in-Aid for Scientific Research (No. 26420486, 26282103).

8. REFERENCES

Akagi, T. (1981) "Effects of Mandrel-Driven sand drains on soft clay", Proc. 10th Int. Conf. Soil Mechanics and Foundation Engineering, Stockholm, Vol. 3, pp581-584.

Asaoka, A. (1978) "Observational procedure of settlement prediction", SOILS AND FOUNDATIONS, Vol. 18, No. 4, pp87-101.

Asaoka, A. and Matsuo, M. (1979) "Bayesian approach to inverse problem in sonsolidation and its application to settlement prediction", Proc. 3rd Int. Conf. Numerical Methods in Geomechanics, Aachen, pp115-123.

Asaoka. A. and Matsuo, M. (1980) "An inverse problem approach to settlement prediction", SOILS AND FOUNDATIONS, Vol. 20, No. 4, pp53-66.

Dumn Muh, J. (1977) "Geotechnical observation from a deep bore hole at Rangsit", AIT Master of Engineering Thesis No. 1004.

Empig, V. E. (1981) "Residual negative pore pressures in undisturbed clay samples", AIT Master of Engineering, Thesis No. GT-80-2.

Galagoda, H. M. M. B. (1981) " Evaluation of subsidence using Asaoka's method – An inverse approach to the problem", AIT Master of Engineering Thesis No. GT-80-3.

Ho, Y. C. (1982) "Mechanical behavior of a trial embankment on Bangkok clay", AIT Master of Engineering Thesis No. GT-81-7.

Iizuka, A. and Ohta, H. (1982) "Deformation analysis of the rectangular embankment on Bangkok clay, Proc. 17th Japan National Conference on Soil Mechanics and Foundation Engineering (Naha), pp165-168.

Iizuka, A. and Ohta, H. (1987) "A determination procedure of input parameters in elasto-viscoplastic finite element analysis", SOILS AND FOUNDATIONS, Vol. 27, No. 3, pp71-87.

Kang, B. H. (1970) "Effects of back pressure on the consolidation behavior of a soft clay", AIT Master of Engineering Thesis No. 343.

Kangsasitiam, M. (1970) "A comparison between oedometer and stress path method s for settlement analysis under undrained loading conditions", AIT Master of Engineering Thesis No. 337.

Kanjanophas, S. (1969) "Compressibility of Bangkok clay in the weathered zone", AIT Master of Engineering Thesis No. 338.

Kim, S. K. (1970) "Pore pressure development during one-dimensional consolidation of soft Bangkok clay", AIT Master of Engineering Thesis No. 339.

Kobayashi, I., Nakayama, E., Iizuka, A. and Ohta, H. (2014) "On the new triaxial testing apparatus- SMART triaxial testing apparatus-", Proc. 59th Symposium on Geotechnical Engineering, pp115-120 (in Japanese)

Ladd, C. C. and Lambe, T. W. (1964) "The strength of "undisturbed" clay determined from undrained tests", Laboratory Shear Testing of Soils, ASTM Special Technical Publication No. 361, pp342-371.

Lambe, T. W. (1964) "Methods of estimating settlements", Jour. of the Soil Mech. And Found. Div., ASCE, Vol. 90, No. SM5, pp43-68.

Mikasa, M. (1965) "The consolidation of soft clay – A new consolidation theory and its applications", Kajima Kenkyusho Shuppankai, Tokyo (in Japanese).

Molla, Md. K. A. (1981) "Secondary consolidation studies on Bangkok clay", AIT Master of Engineering Thesis No. GT-80-16.

Nakayama, E., Kobayashi, I., iizuka, A., Taya, M. and Ohta, H. (2013) "Chapter 22 Development of a portable triaxial testing apparatus –*Smart Triaxial*" , Geotechnical Predictions and Practice in Dealing with Geohazards, edited by Jian Chu, Sri P. R. Wardani and Atsushi Iizuka, Springer, ISSN 1573-6059, ISBN 978-94-007-5674-8, ISBN 978-94-007-5675-5 (e-Book), DOI 10.1007/978-94-007-5675-5, pp353-373.

Noorany, I. and Seed, H. B. (1965) "In-situ strength characteristics of soft clays", Jour. Soil Mech. And Found. Div., ASCE, Vol. 91, No. SM2, pp49-79.

Ohta, H. and Ho, Y. C. (1982) "A trial embankment on soft Bangkok clay, Phase I-Phase III", AIT Research Report, No. RR146.

Pham, Tiem Nam (1972) "Application of the Dutch cone in the Bangkok area", AIT Master of Engineering Thesis No. 377.

Poulos, H. G., de Ambrosis, L. P. and Davis, E. H. (1976) "Method of calculating long-term creep settlements", Jour. Geotech, Engg. Div., ASCE, Vol. 102, No. GT7, pp787-804.

Prapaitrakul, N. (1975) "Settlement of friction piles on soft Bangkok clay", AIT Master of Engineering Thesis No. 771.

Rahman, M. M. M. (1980) "Settlement characteristics of test embankment on soft clay foundation with and without sand drains", AIT Master of Engineering Thesis No. GT-79-15.

Sekiguchi, H. and Ohta, H. (1977) "Induced anisotropy and time dependency in clays", Proc. Specialty Session 9, 9th Int. Conf. on Soil Mech. And Found. Engg, Tokyo, pp475-484.

Skempton, A. W. and Sowa, V. A. (1963) "The behavior of saturated clays during sampling and testing, Geotechnique, Vol. 13, pp256-290.

Taesiri, Y. (1976) "Consolidation characteristics of Rangsit clay", AIT Master of Engineering Thesis No. 918.

Takeyama, T., Ikeda, A., Nakayama, E., Taya, M., Kobayashi, I., Pipatpongsa, T. and Ohta, H. (2014) "Microscopic image of meta-stability of clays", Proc. The TC 105ISSMGE Int. Symposium on Geomechanics from Micro to Macro, Cambridge, CRC Press, Vol. 2, pp727-732.